

Effect of Flexible Spacers on the Rheological Behavior of Main-Chain Thermotropic Liquid-Crystalline Polymers Having Bulky Pendent Side Groups[†]

Sukky Chang and Chang Dae Han*

Department of Polymer Engineering, The University of Akron, Akron, Ohio 44325-0301

Received November 26, 1996; Revised Manuscript Received January 27, 1997[®]

ABSTRACT: The effect of flexible spacers on the rheological behavior of main-chain thermotropic liquid-crystalline polymers having bulky pendent side groups, poly[(phenylsulfonyl)-*p*-phenylenealkylenebis-(4-oxybenzoate)]s (PSHQ_{*n*}), was investigated. For the study we synthesized a homologous series of PSHQ_{*n*} polymers containing methylene groups, varying from 3 to 12, as the flexible spacer and then investigated their transient, steady-state, and oscillatory shear flow behaviors using a cone-and-plate rheometer. We identified the factors which give rise to, during experiment, time-dependent rheological behavior by taking wide-angle X-ray diffraction (WAXD) patterns of the specimen right before and after each rheological measurement. The initial conditions (i.e., the initial morphology) for transient shear flow were controlled by first heating an as-cast specimen to the isotropic region, shearing there at a rate of 0.1 s⁻¹ for ca. 10 min, and then cooling slowly to a preset temperature in the nematic region. Only *positive* values of steady-state first normal stress difference were observed in all the PSHQ_{*n*} polymers synthesized, except for PSHQ₃ having 3 methylene groups of flexible spacer, at all temperatures and shear rates investigated. Interestingly enough, we found that PSHQ₃ exhibits Newtonian behavior at low shear rates over the entire range of temperatures tested, showing *no* evidence of liquid crystallinity from a rheological point of view. This observation is consistent with our earlier findings based on differential scanning calorimetry and WAXD that PSHQ₃ is a glassy, non-liquid-crystalline homopolyester. When steady-state shear viscosity (η) in the nematic region is plotted against $T - T_{NI}$, where T is a measurement temperature and T_{NI} is a clearing temperature, we found that PSHQ_{*n*} moieties with odd numbers of methylene groups have higher values of η in the nematic region compared to PSHQ_{*n*} moieties with even numbers of methylene groups of the flexible spacer.

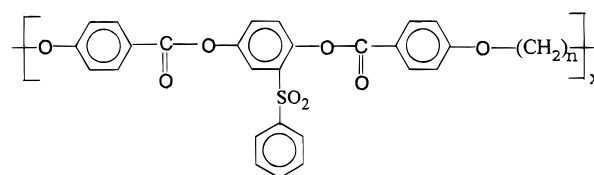
1. Introduction

During the past decade, numerous investigators reported on the rheological behavior of thermotropic liquid-crystalline polymers (TLCPs); namely, some investigators used main-chain thermotropic homopolyesters, and others used thermotropic copolyesters. There are too many papers to cite them all here, and the readers are referred to papers by Han and coworkers^{1,2} and references cited therein. It is clear from the literature that the rheological behavior of TLCP depends very much on thermal and deformation histories, which in turn greatly influence its morphological state. These observations lead us to conclude that the rheological behavior of TLCP is intimately related to its morphological state. Therefore the control of thermal and deformation histories of TLCP specimens is extremely important to obtain reproducible rheological data. Admittedly there can be many different reasons why irreproducible rheological data might be obtained. For instance, it is virtually impossible to obtain reproducible rheological data when the chemical structure of a TLCP is such that its morphological state, via either post polymerization or recrystallization, changes constantly during rheological measurement. This then suggests that one must judiciously choose a TLCP(s), so that its morphological state remains constant during the entire period of rheological measurement. Only such rheological data would be useful to help develop a molecular theory.

To date, there are relatively few studies reported in the literature which describe the effect of chemical

structure on the rheological behavior of TLCPs. Needless to say, there are a very large number of chemical structures which give rise to liquid crystallinity, and thus it is virtually impossible to take rheological measurements for all those TLCPs synthesized so far. One can, however, take a more focused view in that, for instance, main-chain TLCPs having different flexible spacer lengths can be used for such purposes. Even when confining our interest to main-chain TLCPs with flexible spacers, there are a number of chemical structures reported in the literature.^{3,4} However, the majority of the studies reported so far in the literature deal with phase transitions affected by the flexible spacer length and/or by the odd–even nature of flexible spacers,^{3,4} and virtually nothing has been reported on the rheological behavior of main-chain TLCPs affected by the length of flexible spacers and/or by the odd–even nature of the flexible spacers.

As part of our continuing efforts to enhance our understanding of the rheological behavior of main-chain TLCPs, in this study we synthesized a homologous series of poly[(phenylsulfonyl)-*p*-phenylenealkylenebis-(4-oxybenzoate)]s (PSHQ_{*n*}) having methylene groups, ranging from 3 to 12, as the flexible spacer, with chemical structure



and investigated their rheological behaviors, namely, transient, steady-state and oscillatory shear flow behaviors. Throughout this paper, we use the convention

[†] This paper is dedicated to Professor Robert W. Lenz who first reported⁵ on the synthesis of the polymers investigated in this study.

[®] Abstract published in *Advance ACS Abstracts*, March 1, 1997.

of putting “*n*” after an abbreviated name of the polymer (PSHQ) to denote the number of methylene groups of the flexible spacer. In this study we have identified the factors which give rise to, during experiment, time-dependent rheological behavior by taking wide-angle X-ray diffraction (WAXD) patterns of the specimen right before and after each rheological measurement. Using the clearing temperature of each PSHQ n as a reference temperature, we were able to obtain generalized viscosity curves which become independent of the molecular weight of a PSHQ n . We observed a tendency that PSHQs with odd numbers of methylene groups have shear viscosities higher than a PSHQ n with even numbers of methylene groups of the flexible spacer. Possible reasons for this observation will be presented later in this paper. Below we present the highlights of our findings.

2. Experimental Section

Materials and Sample Preparation. We synthesized a homologous series of PSHQ n polymers having methylene groups, ranging from 3 to 12, as the flexible spacer. The details of the synthesis procedures employed are described elsewhere.^{5,6} Specimens for rheological measurements for PSHQ n were prepared by solvent casting and drying in a vacuum oven, the details of which are described in earlier papers of Kim and Han.^{1,7} In the present study, except for PSHQ4 and PSHQ6, all PSHQ n moieties were dissolved in dichloromethane, in the presence of an antioxidant and the solvent was evaporated slowly first at room temperature for a week and then in a vacuum oven at $T_g - 10$ °C for 3 days. Further, specimens were dried in a vacuum oven at ca. $T_m - 10$ °C or $T_g + 10$ °C for 2 h. PSHQ4 and PSHQ6 did not dissolve in dichloromethane, and thus tetrachloroethane was used to dissolve them at an elevated temperature (100 °C) and the specimen was cooled slowly to room temperature, upon which they did not precipitate.

Rheological Measurement. A Rheometrics mechanical spectrometer (RMS Model 800) with a cone-and-plate (8 mm diameter plate, 0.1 radian cone angle) fixture was used to measure: (1) in the transient shear mode, shear stress growth ($\sigma^+(t, \dot{\gamma})$) and first normal stress difference growth ($N_1^+(t, \dot{\gamma})$) as functions of time (t) for various shear rates ($\dot{\gamma}$) and temperatures and (2) in the steady-state shear mode, shear stress (σ), shear viscosity (η), and first normal stress difference (N_1) as functions of shear rate ($\dot{\gamma}$) and temperature. Using a parallel-plate (8 mm diameter plates) fixture, the dynamic storage modulus (G') and dynamic loss modulus (G'') were measured as functions of angular frequency (ω), for which strain amplitude was varied from 0.01 to 0.06, which was well within the linear viscoelastic range of the materials investigated. All experiments were conducted under a nitrogen atmosphere in order to preclude oxidative degradation of the specimen. The temperature control was satisfactory to within ± 1 °C.

Differential Scanning Calorimetry (DSC). The glass transition temperature (T_g) and the clearing temperature (T_{NI}) of all ten PSHQ n polymers synthesized were determined using a differential scanning calorimeter (du Pont 9900) under a nitrogen atmosphere at heating and/or cooling rates of 20 °C/min. Table 1 gives a summary of the T_g and the T_{NI} values of the polymers, in which values of T_{NI} were obtained during the second heating cycle. Also given in Table 1 are the melting point (T_{m2}) of solid crystals, which are formed during polymerization, and the melting point (T_{m1}) of high-temperature melting crystals, which are formed via crystallization during annealing after the melting of solid crystals, for PSHQ n moieties having even numbers of methylene groups. It should be mentioned that values of T_{m1} depend, to some extent, on the annealing conditions employed. As reported in our previous paper,⁸ all PSHQ n moieties having even numbers of methylene groups are crystalline in the solid state and undergo crystalline–nematic and nematic–isotropic transitions, while all PSHQ n moieties having odd numbers of methylene groups

Table 1. Summary of the Transition Temperatures for PSHQ n Investigated in This Study

polymer	T_g (°C)	T_{m2} (°C)	T_{m1} (°C)	T_{NI} (°C)
PSHQ3	129.1	amorphous		^a
PSHQ4	128.2	154.2	240.2 ^b	259.2
PSHQ5	104.1	amorphous		167.7
PSHQ6	109.9	135.5	200.6 ^c	228.0
PSHQ7	92.1	amorphous		171.4
PSHQ8	101.1	128.9	168.5 ^d	198.5
PSHQ9	84.4	amorphous		162.1
PSHQ10	91.8	120.5	151.9 ^e	181.1
PSHQ11	77.1	amorphous		147.0
PSHQ12	84.6	118.0	147.0 ^f	166.9

^a PSHQ3 was found to only undergo a glass transition over the entire range of temperatures investigated, indicating that it is an amorphous thermoplastic. ^b After annealing at 190 °C for 144 h. ^c After annealing at 160 °C for 144 h. ^d After annealing at 130 °C for 144 h. ^e After annealing at 130 °C for 120 h. ^f After annealing at 130 °C for 144 h.

are amorphous in the solid state and only undergo a nematic–isotropic transition (except for PSHQ3). The above observation leads us to conclude that the formation of a well-ordered structure is not possible in PSHQ n moieties having odd numbers of methylene groups, which seems to indicate that the molecular conformation might be quite different between PSHQ n moieties having odd numbers of methylene groups and PSHQ n moieties having even numbers of methylene groups of flexible spacers. Also conducted in the present study were DSC experiments on specimens, which were collected before and after each rheological measurement, in order to investigate whether or not a new phase, via recrystallization, was formed during an isothermal annealing of the specimen in the rheometer.

Wide-Angle X-ray Diffraction (WAXD). WAXD experiments were conducted at room temperature, using a General Electric X-ray generator (Model XRD-6) operated at 30 kV and 30 mA (Ni-filtered Cu K α radiation), on specimens collected (i) right after being squeezed from ca. 1.5 mm to 50 μ m within the cone-and-plate fixture of the rheometer and (ii) after being subjected to an oscillatory shear flow at $\omega = 1$ rad/s for a predetermined period under isothermal conditions. The specimen was cut along the radial direction, which was the major flow direction during squeeze flow, with the width of ca. 1 mm. The purpose of the WAXD experiments performed was to investigate how the squeezing applied to a specimen might have affected the orientations of domain texture during the rheological measurement. The flat plate diffraction patterns were recorded at a distance of 3.23 cm from the specimen, and the exposure time was 2 h.

3. Results and Discussion

We have taken vast amounts of rheological data for 10 PSHQ n moieties having methylene groups, varying from 3 to 12, as the flexible spacer and it is not possible for us to present here all the rheological data obtained. Thus, below we will present some representative rheological data for PSHQ n moieties, putting emphasis on the effects of the flexible spacer length and odd-even nature of the flexible spacer. In particular, we will discuss in detail the rheological behavior of PSHQ3, PSHQ5, PSHQ6, PSHQ11, and PSHQ12. The rationale behind the choice of these PSHQ n moieties for presentation here is as follows. (1) PSHQ3 is chosen because, as reported in our previous paper,⁸ it is a non-liquid-crystalline homopolyester and thus its rheological behavior is distinctly different from the rheological behavior of nine other PSHQ n moieties investigated in this study. (2) A pair of PSHQ5 and PSHQ6 and a pair of PSHQ11 and PSHQ12 moieties are chosen to show the odd-even effect on their rheological behavior. According to our previous study,⁸ PSHQ n moieties having odd numbers of methylene groups (e.g., PSHQ5 and PSHQ11) are glassy nematic homopolyesters which only undergo

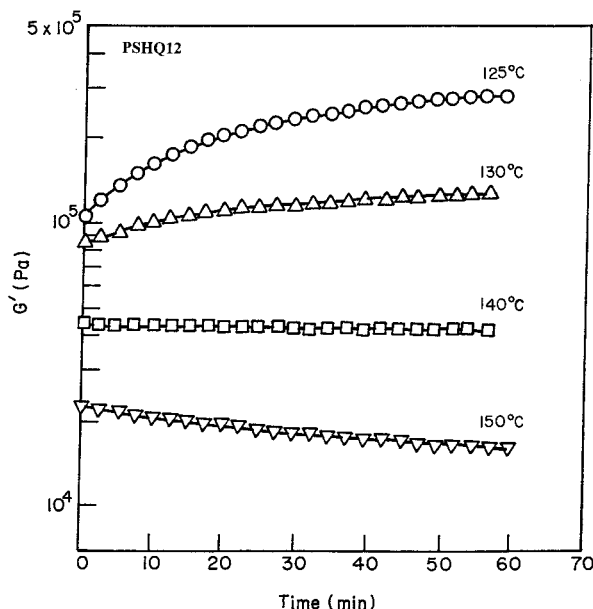


Figure 1. Variations of G' with time at $\omega = 1$ rad/s for as-cast PSHQ12 specimens at various temperatures indicated on the plot.

a nematic–isotropic transition, whereas PSHQ n moieties having even numbers of methylene groups (e.g., PSHQ6 and PSHQ12) undergo both solid–nematic and nematic–isotropic transitions. Because the crystals in PSHQ n having even numbers of the flexible spacer first melt and then recrystallize over a certain range of temperatures, the rheological behavior of PSHQ6 and PSHQ12 was found to be very sensitive to the thermal history of the specimen.

3.1. Variations of G' with Time During Isothermal Annealing of PSHQ n . It was Lin and Winter⁹ who first reported on an increasing trend of G' and G'' with time when a commercial thermotropic copolyester consisting of *p*-hydroxybenzoic acid (HBA) and 6-hydroxy-2-naphthoic acid (HNA) (Vectra A900, Hoechst-Celanese Company) was loaded into the cone-and-plate fixture of the rheometer and then subjected, under isothermal conditions, to an oscillatory shear flow at a low angular frequency. They attributed the increasing trend of G' and G'' observed with time to the postpolymerization process that might have taken place in the presence of unreacted HBA in Vectra A900. Subsequently, a similar observation was reported by Kim and Han⁷ who employed PSHQ10. In their study, however, Kim and Han observed not only an increasing but also a decreasing trend of G' and G'' with time, depending upon the temperature chosen for isothermal annealing; specifically a decreasing trend of G' and G'' with time was observed when the annealing temperature approached the T_{NI} of PSHQ10, which was about 175 °C as determined by DSC. They attributed the increasing trend of G' and G'' observed with time to the formation, via recrystallization, of another form of crystals and the decreasing trend of G' and G'' observed with time to the growth of fine Schlieren texture of the nematic mesophase in the specimen.

In the present study, in conjunction with the low-frequency oscillatory shear flow experiments under isothermal conditions, we employed both DSC and WAXD in order to examine structural changes, if any, in the specimen during rheological experiment.

(A) PSHQ12. Figure 1 describes variations of G' with annealing time up to 60 min at $\omega = 1$ rad/s for

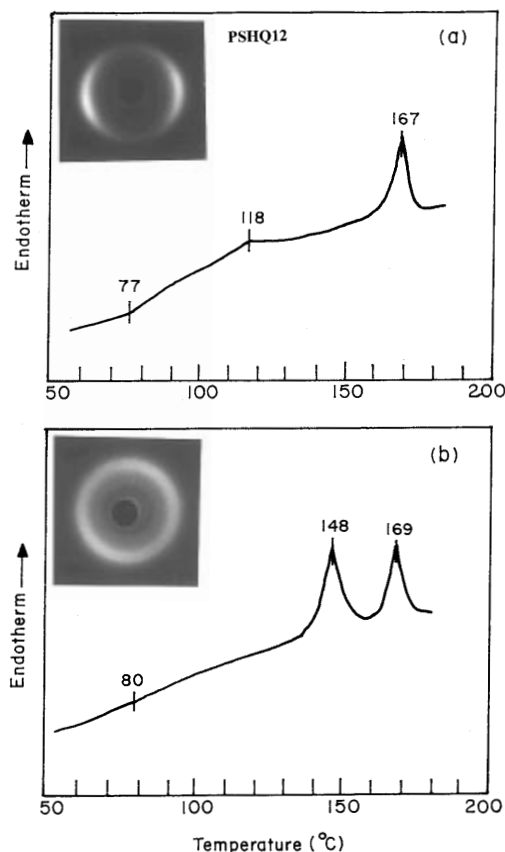


Figure 2. WAXD patterns and DSC traces at a heating rate of 20 °C/min of an as-cast PSHQ12 specimen: (a) right after being squeezed in the cone-and-plate fixture at 125 °C; (b) after being annealed for 1 h at 125 °C under an oscillatory shear flow at $\omega = 1$ rad/s.

as-cast PSHQ12 specimens at 125, 130, 140, and 150 °C. Note that a fresh specimen was used at each temperature. In Figure 1 we observe that values of G' steadily increase with time when a specimen was annealed at 125 °C, stay more or less constant when annealed at 140 °C, but decrease with time when annealed at 150 °C. This seemingly peculiar behavior can be explained using the DSC traces and WAXD patterns presented below.

Figure 2a gives a DSC trace and WAXD patterns of an as-cast PSHQ12 specimen which was collected right after the sample loading into the cone-and-plate fixture which had been preheated at 125 °C and then squeezed from ca. 1.5 mm to 50 μ m. Figure 2b gives a DSC trace and WAXD patterns of a PSHQ12 specimen which was collected after the completion of a low-frequency oscillatory shear flow experiment at 125 °C for 60 min under isothermal conditions. The following observations are worth noting in Figure 2. (1) The PSHQ12 specimen has a T_g of 77 °C, a melting temperature (T_{m2}) of 118 °C, and a T_{NI} of 167 °C. (2) A new crystalline phase, which melts at 148 °C, was created after the PSHQ12 specimen had been annealed at 125 °C for 60 min under oscillatory shear flow. There no longer exists T_{m2} in Figure 2b, suggesting that the crystals melted away at 118 °C during the isothermal annealing at 125 °C and then recrystallization took place, forming high-temperature melting crystals which melt at 148 °C. Hereafter the melting temperature of this new crystal will be denoted by T_{m1} . (3) The WAXD patterns indicate that the specimen was oriented right after the squeezing but the orientation disappeared almost completely after the specimen had been subjected to low-frequency oscilla-

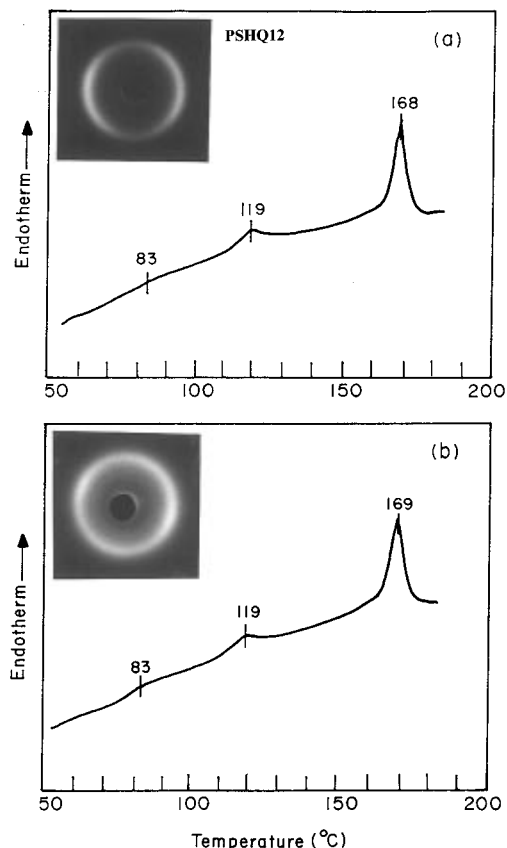


Figure 3. WAXD patterns and DSC traces at a heating rate of 20 °C/min of an as-cast PSHQ12 specimen: (a) right after being squeezed in the cone-and-plate fixture at 150 °C; (b) after being annealed for 1 h at 150 °C under an oscillatory shear flow at $\omega = 1$ rad/s.

tory shear flow at 125 °C for 60 min under isothermal conditions. Therefore we tentatively conclude that an increasing trend of G' with time, observed in Figure 1, was attributable to the formation of high-temperature melting crystals.

Figure 3a gives a DSC trace and WAXD patterns of an as-cast PSHQ12 specimen which was collected right after the sample loading into the cone-and-plate fixture which had been preheated at 150 °C and then squeezed from ca. 1.5 mm to 50 μm . Figure 3b gives a DSC trace and WAXD patterns of a PSHQ12 specimen which was collected after the completion of low-frequency oscillatory shear flow experiment at 150 °C for 60 min under isothermal conditions. In Figure 3 we observe that DSC traces before and after the isothermal annealing at 150 °C for 60 min are the same, indicating that there had been no change in the crystalline structure of PSHQ12 during the isothermal annealing at 150 °C under oscillatory shear flow. This is expected because the annealing temperature of 150 °C is higher than T_{m1} . The WAXD patterns in parts a and b of Figure 3 are essentially the same as those in parts a and b of Figures 2, suggesting that the formation of high-temperature melting crystals, when a specimen was annealed at 125 °C, did not interfere with the relaxation of the orientations introduced by the specimen squeezing. Notice that the WAXD patterns in Figure 2a show more radial orientations than those in Figure 3a, because the specimen squeezed at 125 °C had a higher viscosity than the specimen squeezed at 150 °C and hence the stresses introduced by squeezing would relax at much a slower rate at 125 °C than at 150 °C. Therefore we tentatively conclude that a decreasing trend of G' at 150 °C with

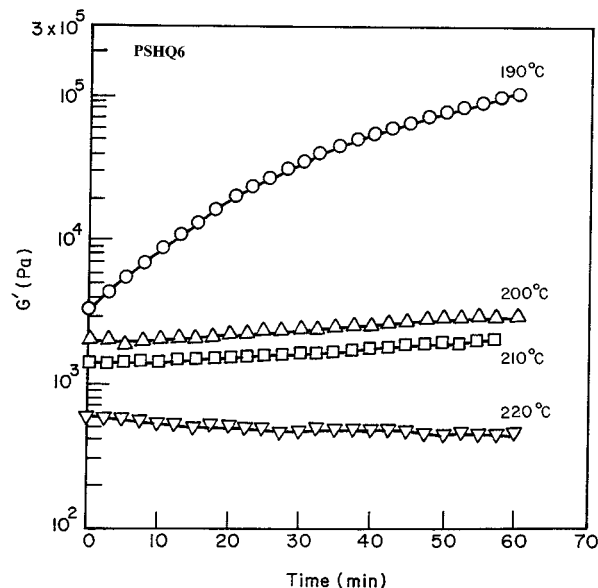


Figure 4. Variations of G' with time at $\omega = 1$ rad/s for as-cast PSHQ6 specimens at various temperatures indicated on the plot.

time, observed in Figure 1, was attributable, in the absence of the formation of high-temperature melting crystals, to the growth of a fine Schlieren-textured nematic mesophase in the specimen. It should be mentioned that earlier, using cross-polarized optical microscopy and light scattering, Kim and Han⁷ have shown that the size of Schlieren textures in PSHQ10 increased with time during isothermal annealing and the growth rate of the Schlieren-textured nematic mesophase increased with increasing annealing temperature.

It is not difficult to imagine that the formation of high-temperature melting crystals would play a dominant role in controlling the growth rate of Schlieren textures, and thus the time evolution of G' (as well as G''), during isothermal annealing. Therefore we can conclude that when an as-cast PSHQ12 specimen was annealed at 125 °C under isothermal conditions (see Figure 2), the formation of high-temperature melting crystals must have overpowered the growth of Schlieren texture in PSHQ12, which otherwise would have given a decreasing trend of G' .

(B) PSHQ6. Figure 4 describes variations of G' , with annealing time up to 60 min at $\omega = 1$ rad/s for as-cast PSHQ6 specimens at 190, 200, 210, and 220 °C. Note that a fresh specimen was used at each temperature. In Figure 4 we observe that values of G' increase very rapidly with time when a specimen was annealed at 190 °C, increase very slowly with time when annealed at 200 and 210 °C, respectively, but decreases very slowly with time when annealed at 220 °C.

Let us look at the DSC traces and WAXD patterns for the PSHQ6 specimens before and after isothermal annealing at various temperatures. Figure 5a gives a DSC trace and WAXD patterns of an as-cast PSHQ6 specimen which was collected right after the sample loading into the cone-and-plate fixture which had been preheated at 190 °C and then squeezed from ca. 1.5 mm to 50 μm . Figure 5b gives a DSC trace and WAXD patterns of a PSHQ6 specimen which was collected after the completion of low-frequency oscillatory shear flow experiment at 190 °C for 60 min under isothermal conditions. The following observations are worth noting in Figure 5. (1) The PSHQ6 specimen has a T_g of 105

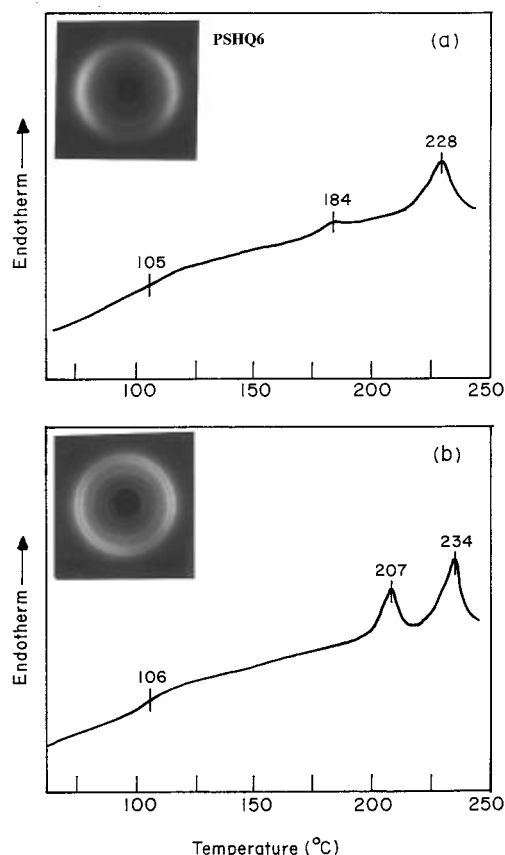


Figure 5. WAXD patterns and DSC traces at a heating rate of 20 °C/min of an as-cast PSHQ6 specimen: (a) right after being squeezed in the cone-and-plate fixture at 190 °C; (b) after being annealed for 1 h at 190 °C under an oscillatory shear flow at $\omega = 1$ rad/s.

°C and a T_{NI} of 228 °C, showing a weak endothermic peak at 184 °C which is too high to be assigned to T_{m2} . (2) After the PSHQ6 specimen had been annealed at 190 °C for 60 min, we observe a very strong endothermic peak appearing at 207 °C below the T_{NI} of 234 °C. We believe that the strong endothermic peak at 207 °C appeared due to the melting or recrystallization of the crystals whose endothermic peak appeared at 184 °C before annealing began. Thus we tentatively conclude that an as-cast PSHQ6 specimen had high-temperature melting crystals even before the specimen was subjected to an isothermal annealing at 190 °C. (3) The above conclusion appears to be supported by the WAXD patterns in Figure 5; specifically the WAXD patterns in Figure 5a have diffuse outer rings, suggesting the melting of the crystals right after the sample loading at 190 °C. Note in Figure 5a that both the outer and inner rings of WAXD patterns are oriented due to squeezing. (4) After the isothermal annealing at 190 °C for 60 min, the WAXD patterns of PSHQ6 specimen show very strong diffraction patterns with several sharp rings, not observed in PSHQ12 (compare Figure 5b with Figure 2b). This observation seems to suggest that the rate of the formation of high-temperature melting crystals is very high in PSHQ6. This observation then seems to explain why the rate of increase of G' with time at 190 °C, given in Figure 4, is very high compared to that at higher temperatures.

Figure 6a gives a DSC trace and WAXD patterns of an as-cast PSHQ6 specimen which was collected right after the sample loading into the cone-and-plate fixture which had been preheated at 220 °C and then squeezed

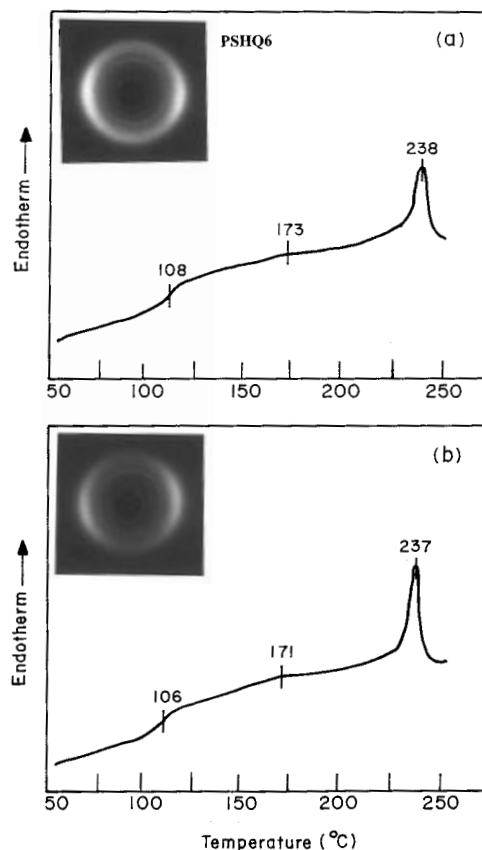


Figure 6. WAXD patterns and DSC traces at a heating rate of 20 °C/min of an as-cast PSHQ6 specimen: (a) right after being squeezed in the cone-and-plate fixture at 220 °C; (b) after being annealed for 1 h at 220 °C under an oscillatory shear flow at $\omega = 1$ rad/s.

from ca. 1.5 mm to 50 μ m. Figure 6b gives a DSC trace and WAXD patterns of a PSHQ6 specimen which was collected after the completion of low-frequency oscillatory shear flow experiment at 220 °C for 60 min under isothermal conditions. In Figure 6 we observe that DSC traces before and after the isothermal annealing at 220 °C for 60 min are essentially the same, indicating that there had been no change in the crystalline structure of PSHQ6 during the isothermal annealing at 220 °C under oscillatory shear flow. The WAXD patterns in Figure 6b indicate that the orientation of the domain texture in the PSHQ6 specimen, which was introduced by the squeezing of the specimen during the sample loading into the cone-and-plate fixture of the rheometer, still persisted after annealing at 220 °C for 60 min, in contrast to the situation for PSHQ12 (compare Figure 6b with Figure 3b). From this observation we can conclude that the orientation of the domain texture in the PSHQ6 specimen is quite stable.

(C) PSHQ5. Figure 7 describes variations of G' with annealing time up to 80 min at $\omega = 1$ rad/s for as-cast PSHQ5 specimens at 125 and 140 °C. Note that a fresh specimen was used for each temperature. In Figure 7 we observe that values of G' stay more or less constant during the entire annealing period at 125 °C, but decrease with time when annealed at 140 °C.

Let us look at the DSC traces and WAXD patterns for the PSHQ5 specimens before and after isothermal annealing at 125 and 140 °C, respectively. Figure 8a gives a DSC trace and WAXD patterns of an as-cast PSHQ5 specimen which was collected right after the sample loading into the cone-and-plate fixture which had been preheated at 125 °C and then squeezed from

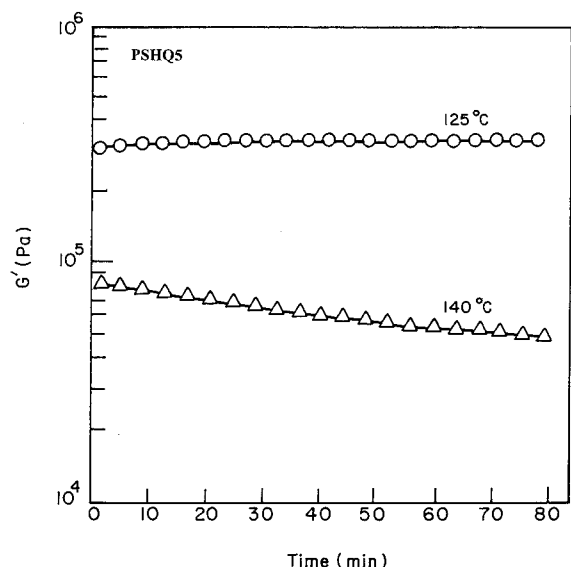


Figure 7. Variations of G' with time at $\omega = 1$ rad/s for as-cast PSHQ5 specimens at various temperatures indicated on the plot.

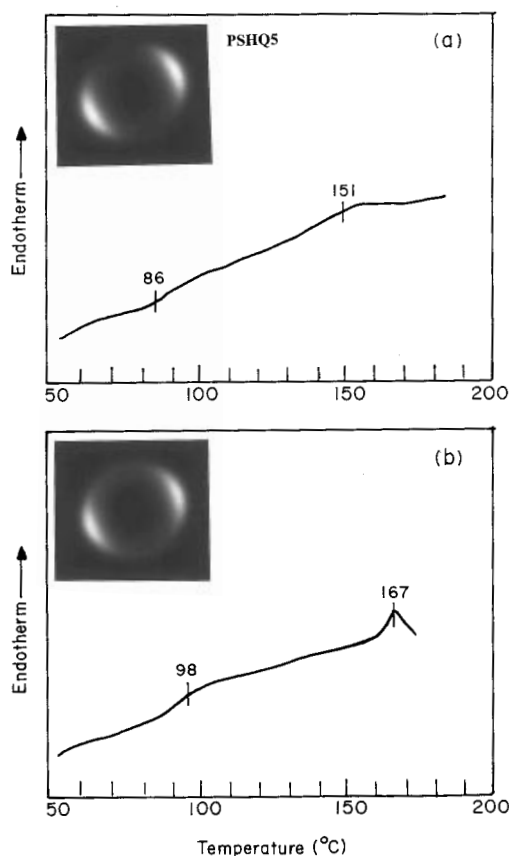


Figure 8. WAXD patterns and DSC traces at a heating rate of 20 °C/min of an as-cast PSHQ5 specimen: (a) right after being squeezed in the cone-and-plate fixture at 125 °C; (b) after being annealed for 80 min at 125 °C under an oscillatory shear flow at $\omega = 1$ rad/s.

ca. 1.5 mm to 50 μ m. Figure 8b gives a DSC trace and WAXD patterns of a PSHQ5 specimen which was collected after the completion of low-frequency oscillatory shear flow experiment at 125 °C for 80 min under isothermal conditions. The following observations are worth noting in Figure 8. (1) The PSHQ5 specimen has only a T_g of 86 °C and a T_{m1} of 151 °C, without showing T_{m2} . (2) After the PSHQ5 specimen had been annealed at 125 °C for 80 min, the characteristics of the DSC trace

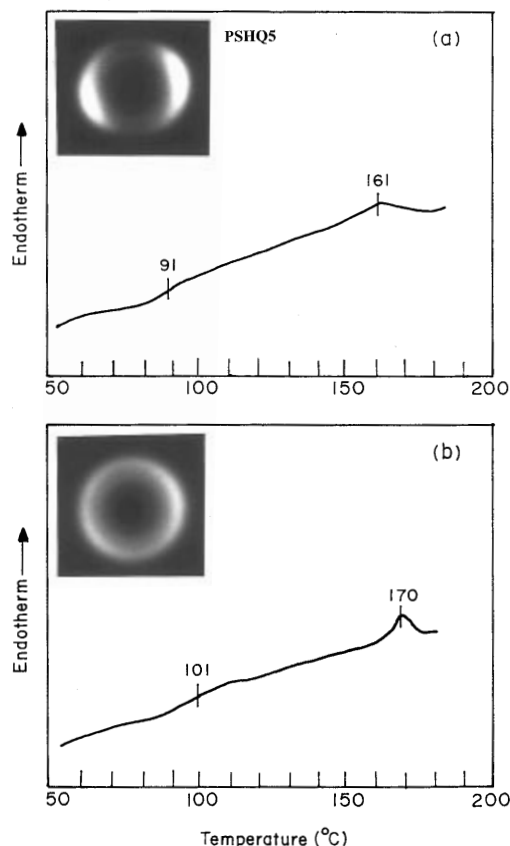


Figure 9. WAXD patterns and DSC traces at a heating rate of 20 °C/min of an as-cast PSHQ5 specimen: (a) right after being squeezed in the cone-and-plate fixture at 140 °C; (b) after being annealed for 80 min at 140 °C under an oscillatory shear flow at $\omega = 1$ rad/s.

remained the same, showing still no evidence of T_{m2} . We thus conclude that PSHQ5 is a glassy TLCP having the nematic mesophase at temperatures between 98 and 167 °C. The constancy of G' with time, shown in Figure 8, when annealed at 125 °C for 80 min, might have been due to the very slow growth rate of the Schlieren-textured nematic mesophase at 125 °C. (3) The WAXD patterns in Figure 8 indicate that the orientation, which had been introduced at the time when the specimen was squeezed, remained almost the same after the isothermal annealing at 125 °C for 80 min. This may be attributable to the very high viscosity of PSHQ5 at 125 °C. This observation then explains why values of G' varied little when annealed at 125 °C, because the growth of domain texture might have been very difficult at 125 °C.

Figure 9a gives a DSC trace and WAXD patterns of an as-cast PSHQ5 specimen which was collected right after the sample loading into the cone-and-plate fixture, which had been preheated at 140 °C and then squeezed from ca. 1.5 mm to 50 μ m. Figure 9b gives a DSC trace and WAXD patterns of a PSHQ5 specimen which was collected after the completion of low-frequency oscillatory shear flow experiment at 140 °C for 80 min under isothermal conditions. In Figure 9 we observe that DSC traces before and after the isothermal annealing at 140 °C for 80 min under oscillatory shear flow are essentially the same, except for an increase of ca. 10 °C in both T_g and T_{m1} due to annealing. The WAXD patterns in parts a and b of Figure 9 indicate that considerable amounts of orientation of domain texture were lost after the specimen had been annealed at 140 °C for 80 min, in contrast to the situation where the specimen was

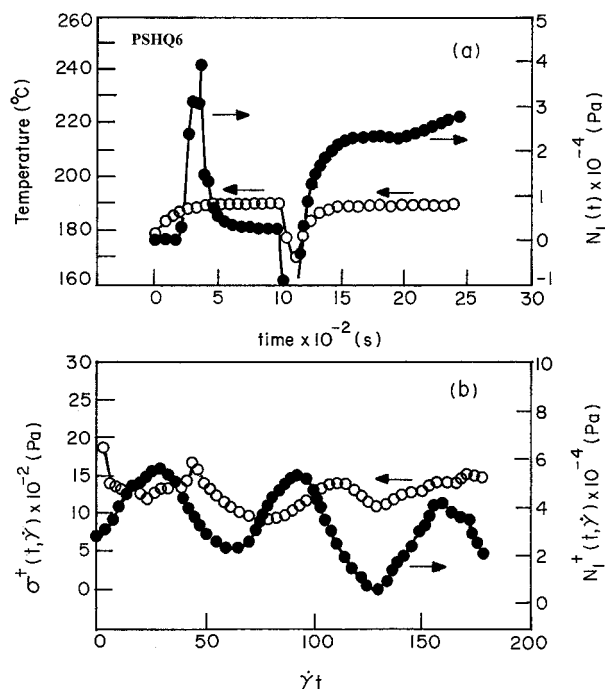


Figure 10. (a) Temperature (○) and N_1 (●) during the loading of an as-cast PSHQ6 specimen onto the cone-and-plate fixture, which was preheated at 190 °C, and (b) plots of $\sigma^+(t, \dot{\gamma})$ vs $\dot{\gamma}t$ (○) and $N_1^+(t, \dot{\gamma})$ vs $\dot{\gamma}t$ (●) at 190 °C and $\dot{\gamma} = 0.1 \text{ s}^{-1}$ after temperature equilibration at 190 °C. Note that the experimental temperature of 190 °C is lower than the T_{m1} (197 °C) of PSHQ6.

annealed at 125 °C. This might have been due to the easier mobility of the chains (i.e., due to low viscosity) of PSHQ5 at 140 °C. The above observation can now explain why values of G' decreased markedly with time, shown in Figure 7, during annealing at 140 °C for 80 min under oscillatory shear flow.

3.2. Transient Shear Flow Behavior of PSHQn.

It is clear from the results presented above that the initial condition (i.e., the initial morphology) of a PSHQn specimen greatly influences its rheological responses; for instance, whether a specimen is loaded into the cone-and-plate fixture of a rheometer at temperatures below or above the T_{m1} , if it exists, would make a great difference in the rheological responses. This can be further illustrated below for transient shear flow experiments.

Figure 10a describes how N_1 of an as-cast PSHQ6 specimen at rest varies with time for a period of 2400 s after the specimen was loaded into the cone-and-plate fixture which had been preheated at 190 °C, and Figure 10b gives plots of $\sigma^+(t, \dot{\gamma})$ and $N_1^+(t, \dot{\gamma})$ vs $\dot{\gamma}t$ after a step shear flow at $\dot{\gamma} = 0.1 \text{ s}^{-1}$ was applied to the specimen. The following observations are worth noting in Figure 10: (a) before a step shear flow was applied, N_1 of the specimen kept increasing with time even after the temperature equilibrated at 190 °C (see the upper panel), indicating that the specimen had *unrelaxed* normal forces; (b) after a step shear flow at $\dot{\gamma} = 0.1 \text{ s}^{-1}$ was applied, both $\sigma^+(t, \dot{\gamma})$ and $N_1^+(t, \dot{\gamma})$ of the specimen exhibited large oscillatory behavior (see the lower panel). This undesirable feature arose, we believe, from the formation of high-temperature melting crystals during sample loading and also during rest after the sample loading, because the experimental temperature of 190 °C was lower than T_{m1} (see Figure 5b). The oscillatory behavior in $N_1^+(t, \dot{\gamma})$ observed in the lower panel of Figure 10 might have originated from the

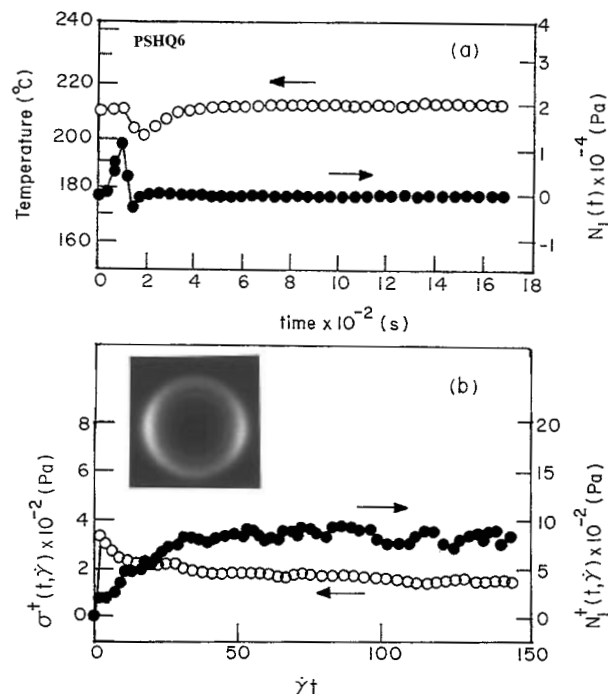


Figure 11. (a) Temperature (○) and N_1 (●) during the loading of an as-cast PSHQ6 specimen onto the cone-and-plate fixture, which was preheated at 210 °C; (b) plots of $\sigma^+(t, \dot{\gamma})$ vs $\dot{\gamma}t$ (○) and $N_1^+(t, \dot{\gamma})$ vs $\dot{\gamma}t$ (●) at 210 °C and $\dot{\gamma} = 0.1 \text{ s}^{-1}$ after temperature equilibration at 210 °C, and WAXD patterns which were taken at room temperature of a specimen which was removed from the rheometer right after the specimen had been squeezed (i.e., before a sudden shear flow was applied to the specimen). Note that the experimental temperature of 210 °C is higher than the T_{m1} (197 °C) of PSHQ6.

slippage between the polymer and the contact metal surface of the cone-and-plate fixture.

However, as can be seen in Figure 11, when an as-cast PSHQ6 specimen was loaded into the cone-and-plate fixture which had been preheated at 210 °C, which is between T_{m1} and T_{NI} (see Figure 5b), we observe that (a) before a step shear flow was applied, N_1 of the specimen at rest attained zero value (see the upper panel) and (b) after a step shear flow at $\dot{\gamma} = 0.1 \text{ s}^{-1}$ was applied, $\sigma^+(t, \dot{\gamma})$ of the specimen went through a maximum and then leveled off to a constant value, while $N_1^+(t, \dot{\gamma})$ of the specimen increased steadily with time without an overshoot and then leveled off with oscillatory behavior (see the lower panel).

Figure 12a gives the temperature protocol employed and describes how N_1 of an as-cast PSHQ6 specimen at rest varies with time after the specimen was first loaded into the cone-and-plate fixture which had been preheated at 240 °C in the isotropic region and then cooled slowly to 210 °C in the nematic region. Figure 12b gives plots of $\sigma^+(t, \dot{\gamma})$ and $N_1^+(t, \dot{\gamma})$ vs $\dot{\gamma}t$ after a step shear flow at $\dot{\gamma} = 0.1 \text{ s}^{-1}$ was applied to the specimen. The following observations are noteworthy in Figure 12: (a) before a step shear flow was applied to the specimen, N_1 of the specimen leveled off to zero value after the temperature equilibrated at 210 °C (see the upper panel), and (b) after a step shear flow at $\dot{\gamma} = 0.1 \text{ s}^{-1}$ was applied, $\sigma^+(t, \dot{\gamma})$ of the specimen exhibited an overshoot and then leveled off to a constant value and $N_1^+(t, \dot{\gamma})$ of the specimen exhibited multiple overshoots. Comparison of Figures 12 and 11 reveals that although both thermal histories give rise to zero values of N_1 before a step shear flow is applied, the two specimens, each having different thermal histories, gave rise to

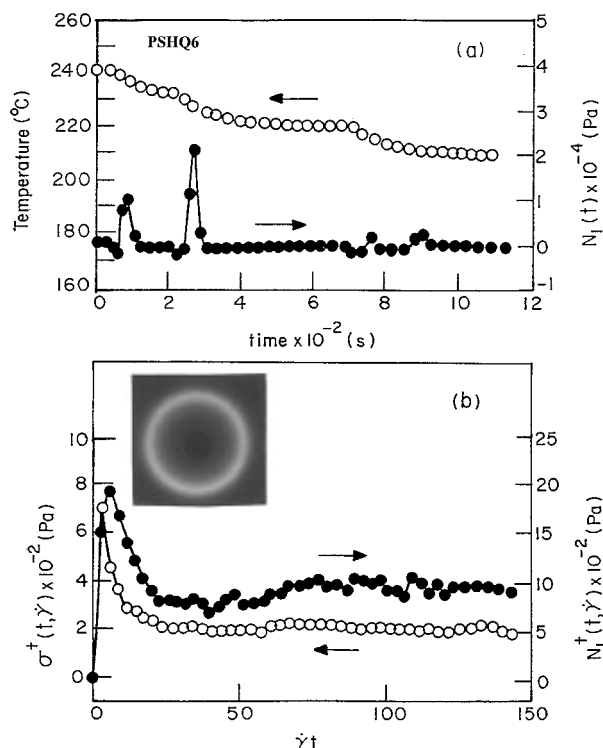


Figure 12. (a) Temperature (○) and N_1 (●) during the cooling from 240 °C to 210 °C after an as-cast PSHQ6 specimen was loaded and squeezed onto the cone-and-plate fixture at 240 °C in the isotropic region ($T_{NI} = 228$ °C); (b) plots of $\sigma^+(t, \dot{\gamma})$ vs $\dot{\gamma}t$ (○) and $N_1^+(t, \dot{\gamma})$ vs $\dot{\gamma}t$ (●) at 210 °C and $\dot{\gamma} = 0.1$ s $^{-1}$ after temperature equilibration at 210 °C, and WAXD patterns which were taken at room temperature of a specimen which was removed from the rheometer after the specimen had been squeezed at 240 °C in the isotropic region and then cooled slowly to 210 °C in the nematic region (i.e., before a sudden shear flow was applied to the specimen). Note that the experimental temperature of 210 °C is higher than the $T_{m1} = 197$ °C of PSHQ6.

distinctly different $N_1^+(t, \dot{\gamma})$ behavior. This, we believe, is due to the differences in the initial conditions that existed between the two specimens before a sudden shear flow was applied, as evidenced by the WAXD patterns given in Figures 11b and 12b, i.e., the WAXD patterns in Figure 11b show orientations of domain texture in the specimen which were introduced by squeezing, while the WAXD patterns in Figure 12b show no orientation of domain texture in the specimen. The WAXD patterns given in Figure 11b were taken at room temperature of a specimen that was removed from the rheometer right after it had been loaded and squeezed onto the cone-and-plate fixture at 210 °C in the nematic region. On the other hand, the WAXD patterns given in Figure 12b were taken at room temperature of a specimen that was removed from the rheometer after the specimen had been loaded and squeezed onto the cone-and-plate fixture at 240 °C in the isotropic region and then cooled slowly to 210 °C in the nematic region. Notice in Figures 11b and 12b that steady-state values of N_1 are virtually the same, while the $N_1^+(t, \dot{\gamma})$ behavior is quite different, between the two situations.

Figure 13 describes that when an as-cast PSHQ5 specimen was loaded into the cone-and-plate fixture which had been preheated at 150 °C, (a) before a step shear flow was applied, N_1 of the specimen at rest attained zero value (see the upper panel) and (b) after a step shear flow at $\dot{\gamma} = 0.1$ s $^{-1}$ was applied, the $\sigma^+(t, \dot{\gamma})$ of the specimen went through a maximum and then leveled off to a constant value, while the $N_1^+(t, \dot{\gamma})$ first

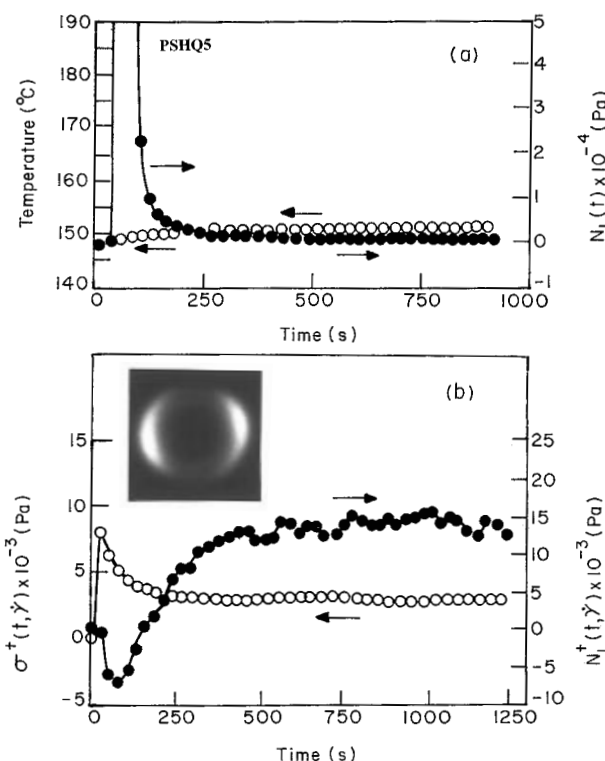


Figure 13. (a) Temperature (○) and N_1 (●) during the loading of an as-cast PSHQ5 specimen onto the cone-and-plate fixture, which was preheated at 150 °C; (b) plots of $\sigma^+(t, \dot{\gamma})$ vs $\dot{\gamma}t$ (○) and $N_1^+(t, \dot{\gamma})$ vs $\dot{\gamma}t$ (●) at 150 °C and $\dot{\gamma} = 0.1$ s $^{-1}$ after temperature equilibration at 150 °C, and WAXD patterns which were taken at room temperature of a specimen which was removed from the rheometer right after the specimen had been squeezed at 150 °C (i.e., before a sudden shear flow was applied to the specimen). Note that PSHQ5 forms a glassy nematic mesophase⁸ and thus it has no T_{m1} .

went through negative values and then increased steadily with time without an overshoot and then leveled off with oscillatory behavior (see the lower panel).

Figure 14a describes the temperature protocol employed and describes how N_1 of an as-cast PSHQ5 specimen, having a T_{NI} of ca. 165 °C, varies with time during rest after the specimen was first loaded into the cone-and-plate fixture which had been preheated at 178 °C in the isotropic region and then cooled slowly down to 150 °C in the nematic region. Figure 14b gives plots of $\sigma^+(t, \dot{\gamma})$ and $N_1^+(t, \dot{\gamma})$ vs $\dot{\gamma}t$ after a step shear flow at $\dot{\gamma} = 0.1$ s $^{-1}$ was applied to the specimen. The following observations are noteworthy in Figure 14: (a) before a step shear flow was applied to the specimen, N_1 of the specimen leveled off to zero value after the temperature equilibrated at 150 °C (see the upper panel), and (b) after a step shear flow at $\dot{\gamma} = 0.1$ s $^{-1}$ was applied, $\sigma^+(t, \dot{\gamma})$ of the specimen exhibited a large overshoot and then leveled off to a constant value. Comparison of Figure 14b and Figure 13b reveals that the two specimens, each having different thermal histories, gave rise to distinctly different $N_1^+(t, \dot{\gamma})$ behavior, which is attributable to the differences in the initial condition that existed between the two specimens before a sudden shear flow was applied, as evidenced by the WAXD patterns given in Figures 13b and 14b.

Figure 15a describes how N_1 of an as-cast PSHQ11 specimen at rest varies with time for a period of 1400 s after the specimen was loaded into the cone-and-plate fixture which had been preheated at 130 °C, and Figure 15b gives plots of $\sigma^+(t, \dot{\gamma})$ and $N_1^+(t, \dot{\gamma})$ vs $\dot{\gamma}t$ after a step

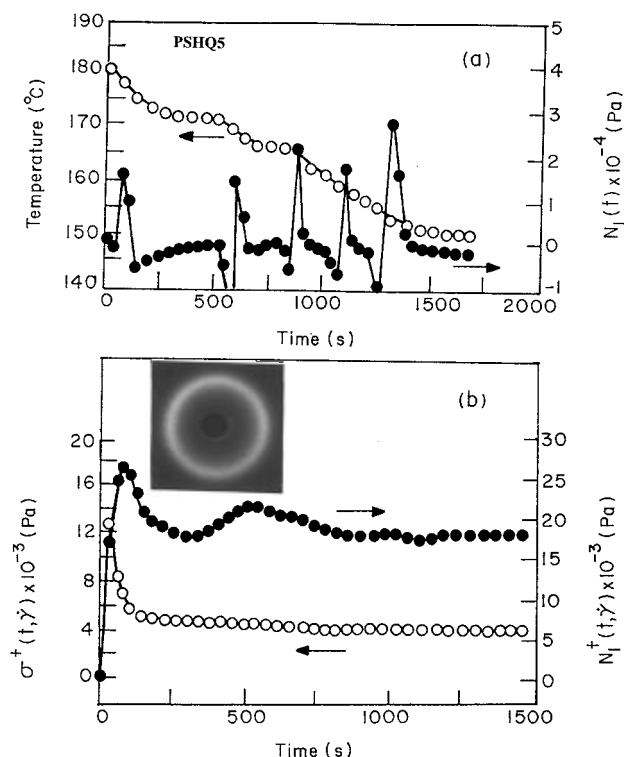


Figure 14. (a) Temperature (○) and N_1 (●) during the cooling from 178 °C to 150 °C after an as-cast PSHQ5 specimen was loaded and squeezed onto the cone-and-plate fixture at 178 °C in the isotropic region ($T_{NI} = 165$ °C); (b) plots of $\sigma^+(t, \dot{\gamma})$ vs $\dot{\gamma}t$ (○) and $N_1^+(t, \dot{\gamma})$ vs $\dot{\gamma}t$ (●) at 150 °C and $\dot{\gamma} = 0.1$ s $^{-1}$ after temperature equilibration at 150 °C and WAXD patterns which were taken at room temperature of a specimen which was removed from the rheometer after the specimen had been squeezed at 178 °C in the isotropic region and then cooled slowly to 150 °C in the nematic region (i.e., before a sudden shear flow was applied to the specimen). Note that PSHQ5, after first being heated to the isotropic region and then cooled slowly to the nematic region, forms a glassy nematic mesophase⁸ and thus it has no T_{m1} .

shear flow at $\dot{\gamma} = 0.1$ s $^{-1}$ was applied to the specimen. Also given in Figure 15b are WAXD patterns taken at room temperature of a specimen that was removed from the rheometer right after the specimen loading and squeezing at 130 °C. In Figure 15b we observe that $N_1^+(t, \dot{\gamma})$ initially increases without exhibiting an overshoot and then levels off with small oscillations, while $\sigma^+(t, \dot{\gamma})$ exhibits an overshoot before reaching a steady-state value.

Figure 16a describes the temperature protocol employed and variations of N_1 of an as-cast PSHQ11 specimen at rest after it was loaded into the cone-and-plate fixture, which had been preheated at 170 °C in the isotropic region and then cooled slowly to 130 °C in the nematic region. Figure 16b gives plots of $\sigma^+(t, \dot{\gamma})$ and $N_1^+(t, \dot{\gamma})$ vs $\dot{\gamma}t$ after a step shear flow at $\dot{\gamma} = 0.1$ s $^{-1}$ was applied to the specimen. Also given in Figure 16b are WAXD patterns taken at room temperature of a specimen that was removed from the rheometer after the specimen attained temperature equilibration at 130 °C and before a sudden shear flow was applied. The following observations are noteworthy in Figure 16: (a) before a step shear flow was applied to the specimen, N_1 of the specimen leveled off to zero value after the temperature equilibrated at 130 °C (see the upper panel), and (b) after a step shear flow at $\dot{\gamma} = 0.1$ s $^{-1}$ was applied, $\sigma^+(t, \dot{\gamma})$ of the specimen exhibited an overshoot and then leveled off to a constant value and $N_1^+(t, \dot{\gamma})$ of the specimen exhibited a large overshoot

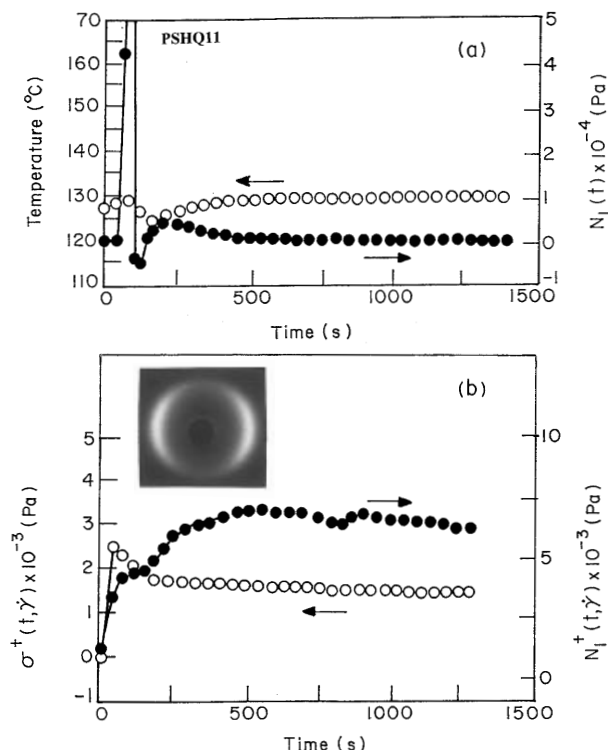


Figure 15. (a) Temperature (○) and N_1 (●) during the loading of an as-cast PSHQ11 specimen onto the cone-and-plate fixture, which was preheated at 130 °C; (b) plots of $\sigma^+(t, \dot{\gamma})$ vs $\dot{\gamma}t$ (○) and $N_1^+(t, \dot{\gamma})$ vs $\dot{\gamma}t$ (●) at 130 °C and $\dot{\gamma} = 0.1$ s $^{-1}$ after temperature equilibration at 130 °C, and WAXD patterns which were taken at room temperature of a specimen which was removed from the rheometer right after the specimen had been squeezed at 130 °C (i.e., before a sudden shear flow was applied to the specimen). Note that an as-cast PSHQ11 specimen forms high-temperature melting crystals at ca. 120 °C but such crystals do not appear again in the nematic region once they were melted away by being heated to the isotropic region.⁸ Thus the experimental temperature of 130 °C employed in this experiment is higher than the T_{m1} (120 °C) of as-cast PSHQ11 specimen.

(see the lower panel). Comparison of Figures 16 and 15 reveals, although both specimens yielded zero values of N_1 before a step shear flow was applied, that the two specimens having different thermal histories gave rise to distinctly different $N_1^+(t, \dot{\gamma})$ behavior. Notice further the differences in WAXD patterns in the two specimens, given in Figures 15b and 16b, showing that the specimen that was squeezed in the isotropic region followed by cooling to the nematic region has uniform distribution of domain texture, whereas the specimen that was squeezed in the nematic region has large orientations of domain texture. Thus, we conclude that the large difference in $N_1^+(t, \dot{\gamma})$ behavior upon applying a sudden shear flow, observed in Figures 15b and 16b, is attributable to the differences in the initial conditions that existed between the two specimens before a sudden shear flow was applied. We observed similar transient shear flow behavior for other PSHQ n moieties synthesized in this study. However, one very important conclusion that can be drawn from Figures 11–16 is that an attainment of zero value of normal force before applying a sudden shear flow to PSHQ n specimen is necessary, but not sufficient, for one to have an accurate and reproducible transient shear flow response in $N_1^+(t, \dot{\gamma})$.

Figure 17 describes the effect of shear rate on $\sigma^+(t, \dot{\gamma})$, and Figure 18 describes the effect of shear rate on $N_1^+(t, \dot{\gamma})$, for PSHQ5 at 150 °C. In obtaining these results,

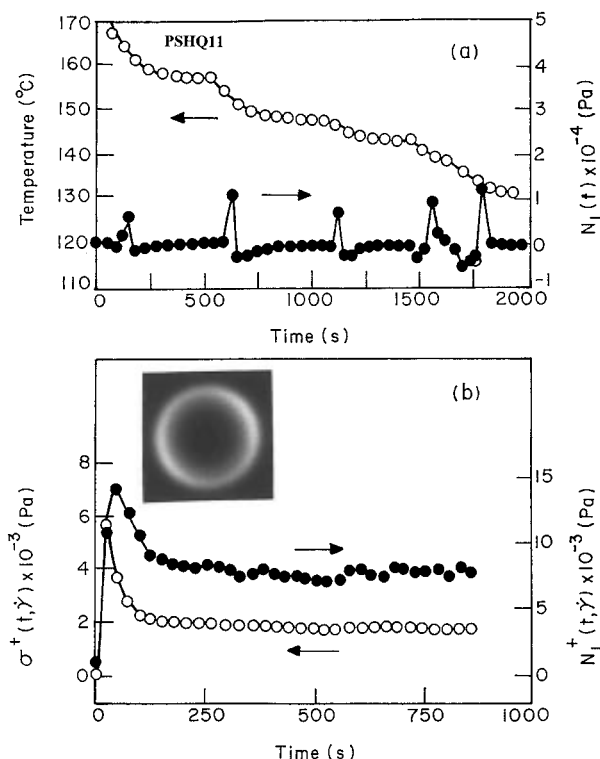


Figure 16. (a) Temperature (○) and N_1 (●) during the cooling from 170 °C to 130 °C after an as-cast PSHQ11 specimen was loaded and squeezed onto the cone-and-plate fixture at 170 °C in the isotropic region ($T_{NI} = 155$ °C); (b) plots of $\sigma^+(t, \dot{\gamma})$ vs $\dot{\gamma}t$ (○) and $N_1^+(t, \dot{\gamma})$ vs $\dot{\gamma}t$ (●) at 130 °C and $\dot{\gamma} = 0.1 \text{ s}^{-1}$ after temperature equilibration at 130 °C, and WAXD patterns which were taken at room temperature of a specimen which was removed from the rheometer after the specimen had been squeezed at 170 °C in the isotropic region and then cooled slowly to 130 °C in the nematic region (i.e., before a sudden shear flow was applied to the specimen). Note that PSHQ11, after first being heated to the isotropic region and then cooled slowly to the nematic region, forms a glassy nematic mesophase⁸ and thus it has no T_{m1} .

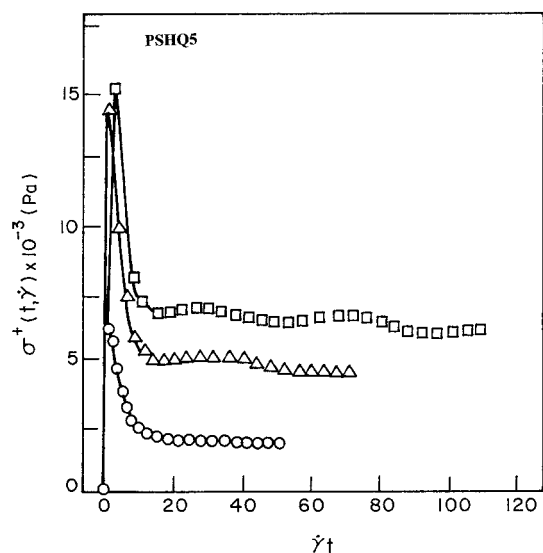


Figure 17. Plots of $\sigma^+(t, \dot{\gamma})$ vs $\dot{\gamma}t$ for as-cast PSHQ5 specimens at 150 °C for different values of $\dot{\gamma}$: (○) 0.1 s⁻¹; (Δ) 0.3 s⁻¹; (□) 0.5 s⁻¹. A fresh specimen was used for each temperature. Each specimen, before being subjected to startup shear flow, was heated to 178 °C in the isotropic region, sheared there at 0.1 s⁻¹ for 10 min, and then cooled slowly to 150 °C in the nematic region.

a fresh specimen was used for each shear rate and the specimen was first heated to 178 °C in the isotropic

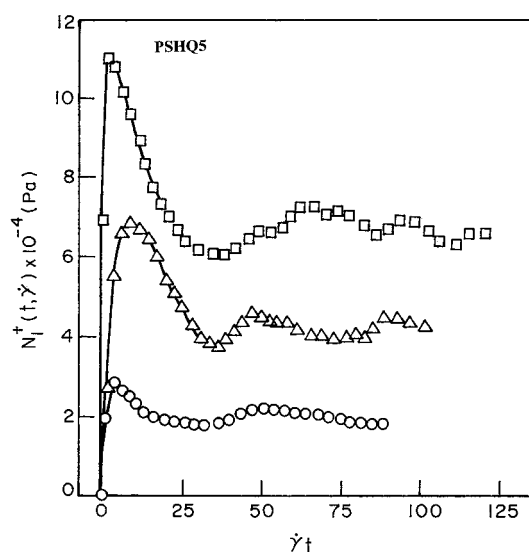


Figure 18. Plots of $N_1^+(t, \dot{\gamma})$ vs $\dot{\gamma}t$ for as-cast PSHQ5 specimens at 150 °C for different values of $\dot{\gamma}$: (○) 0.1 s⁻¹; (Δ) 0.3 s⁻¹; (□) 0.5 s⁻¹. A fresh specimen was used for each temperature. Each specimen, before being subjected to startup shear flow, was heated to 178 °C in the isotropic region, sheared there at 0.1 s⁻¹ for 10 min, and then cooled slowly to 150 °C in the nematic region.

region and then cooled slowly to 150 °C in the nematic region. Note that the T_{NI} of PSHQ5 is ca. 167 °C (see Table 1). In Figure 17 we observe that the magnitudes of both the overshoot in $\sigma^+(t, \dot{\gamma})$ and the steady-state shear stress (σ) increase with increasing $\dot{\gamma}$ from 0.1 to 0.5 s⁻¹. Similarly, in Figure 18 we observe that the magnitudes of both the overshoot in $N_1^+(t, \dot{\gamma})$ and the steady-state first normal stress difference (N_1) increase with increasing $\dot{\gamma}$ from 0.1 to 0.5 s⁻¹. However, we observe multiple overshoots in $N_1^+(t, \dot{\gamma})$, which is believed to be characteristic of liquid-crystalline polymers in general.^{1,2,10,11} It should be mentioned that we made observations, similar to Figures 17 and 18, for other PSHQ n moieties synthesized in this study.

It is noteworthy to mention that the unusually large values of overshoot in $\sigma^+(t, \dot{\gamma})$ and $N_1^+(t, \dot{\gamma})$ observed in Figures 17 and 18 are believed to be characteristics of TLCPs in general. From a rheological point of view, such large overshoots in $\sigma^+(t, \dot{\gamma})$ and $N_1^+(t, \dot{\gamma})$ arise from the presence of polydomains in the TLCP specimen. To date, very little overshoot in $\sigma^+(t, \dot{\gamma})$ and $N_1^+(t, \dot{\gamma})$, if any, has been reported on non-liquid-crystalline polymers at such low $\dot{\gamma}$, e.g. $\dot{\gamma} \leq 0.5 \text{ s}^{-1}$. Moreover, in Figures 17 and 18 we observe that the ratio of peak values of $N_1^+(t, \dot{\gamma})$ and $\sigma^+(t, \dot{\gamma})$, $N_{1,\text{max}}/\sigma_{\text{max}}$, and the ratio of the steady-state normal stress difference and shear stress, N_1/σ , are ca. 2–3 at such low $\dot{\gamma}$. On the other hand, such ratios are much less than 0.5 for non-liquid-crystalline polymers at comparable $\dot{\gamma}$. We thus conclude that large values of $N_{1,\text{max}}/\sigma_{\text{max}}$ and N_1/σ are again the characteristics of TLCPs in general. It should be mentioned that only positive values of N_1 were obtained for all PSHQ n moieties investigated in this study. Earlier, similar observations were reported by other investigators.^{1,2,12,13}

3.3. Steady-State Shear Flow Properties of PSHQ n . Figure 19 gives plots of the logarithm of steady-state shear viscosity ($\log \eta$) vs temperature at $\dot{\gamma} = 0.1 \text{ s}^{-1}$ for ten PSHQ n synthesized in this study. It can be seen in Figure 19 that each polymer, with the exception of PSHQ3, shows a minimum and also a maximum in η at a critical temperature. Earlier, similar behavior was reported for other types of TL-

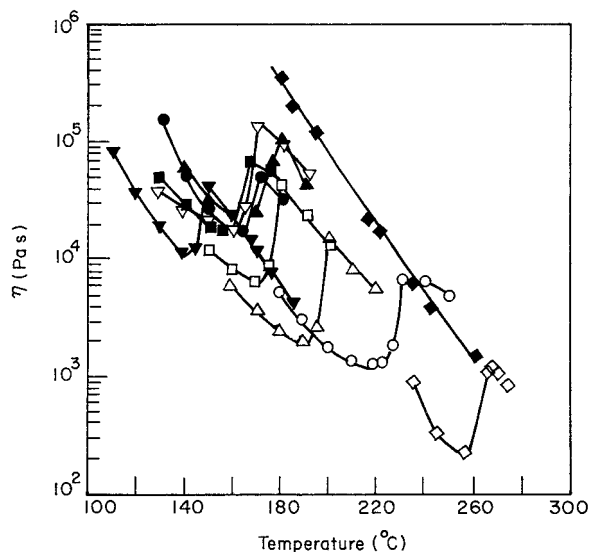


Figure 19. Plots of η vs temperature at $\dot{\gamma} = 0.1 \text{ s}^{-1}$: (◆) PSHQ3; (●) PSHQ5; (▲) PSHQ7; (■) PSHQ9; (▼) PSHQ11; (◇) PSHQ4; (○) PSHQ6; (△) PSHQ8; (□) PSHQ10; (▽) PSHQ12.

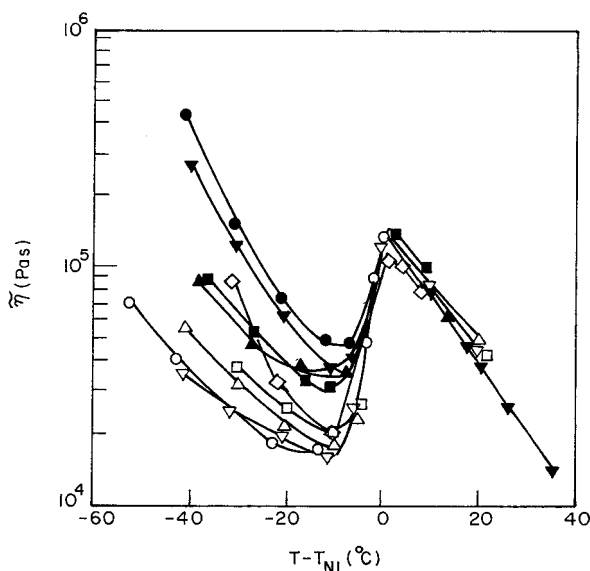


Figure 20. Plots of $\tilde{\eta}$ vs $T - T_{NI}$ at $\dot{\gamma} = 0.1 \text{ s}^{-1}$: (●) PSHQ5; (▲) PSHQ7; (■) PSHQ9; (▼) PSHQ11; (◇) PSHQ4; (○) PSHQ6; (△) PSHQ8; (□) PSHQ10; (▽) PSHQ12.

CPs.^{14,15} In Figure 19 we observe that (1) a decrease of η before reaching a minimum with increasing temperature occurs in the nematic region, (2) an increase of η before reaching a maximum with increasing temperature occurs in the biphasic region, (3) a maximum value of η occurs at T_{NI} , and (4) a decrease of η after passing a maximum with increasing temperature occurs in the isotropic region.

Since Figure 19 sheds little light on the dependence of η on flexible spacer length and the odd-even nature of PSHQ n , we prepared plots of $\tilde{\eta}$ vs $T - T_{NI}$, shown in Figure 20, where values of $\tilde{\eta}$ are the viscosities which were obtained by vertically shifting the maximum value of η for other PSHQ n moieties to the maximum value of η for PSHQ12 as a reference. In view of the fact that T_{NI} reflects the chemical structures of polymers and, also, depends on their molecular weights,¹⁶ plots of $\tilde{\eta}$ vs $T - T_{NI}$, given in Figure 20, can be regarded as being independent of the molecular weights of PSHQ n moieties. Interestingly enough, in Figure 20 we observe a tendency that in the nematic region, values of $\tilde{\eta}$ are

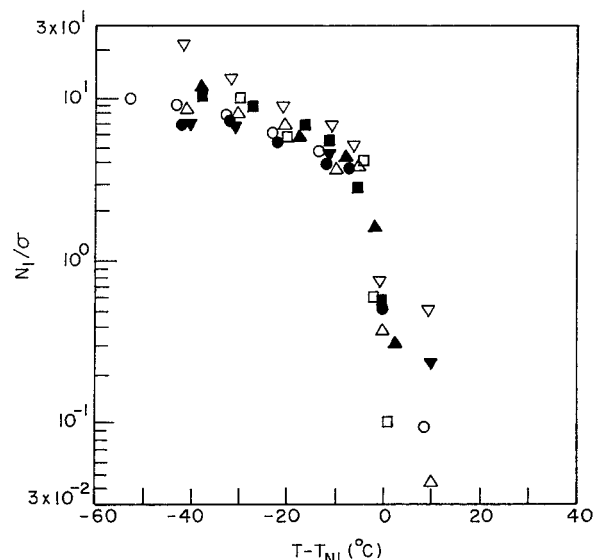


Figure 21. Plots of N_l/σ vs $T - T_{NI}$ at $\dot{\gamma} = 0.1 \text{ s}^{-1}$: (●) PSHQ5; (▲) PSHQ7; (■) PSHQ9; (▼) PSHQ11; (○) PSHQ6; (△) PSHQ8; (□) PSHQ10; (▽) PSHQ12.

much greater for PSHQ n moieties having odd numbers of methylene groups compared to PSHQ n having even numbers of methylene groups of the flexible spacer. In Figure 20 we have not included the η data for PSHQ3 for the obvious reason that it has no T_{NI} .⁸ Such an observation, if it has a generality, seems to suggest that the molecular mobility in the nematic region might be much more difficult in PSHQ n moieties having odd numbers of methylene groups than in PSHQ n moieties having even numbers of methylene groups of the flexible spacer. Such speculation suggests further that the molecular conformation in the nematic state might be quite different between PSHQ n moieties having odd numbers of methylene groups and PSHQ n moieties having even numbers of methylene groups of the flexible spacer.

On the basis of the conformational analyses performed by Abe,¹⁷ at present we can only speculate that the rigid cores of PSHQ n moieties having even numbers of methylene groups may be aligned along one preferred domain axis, while the rigid cores of PSHQ n moieties having odd numbers of methylene groups may be aligned in more than one direction, requiring more energy dissipation during flow. This can be tested by investigating the molecular conformation of PSHQ n moieties using solid-state magnetic resonance spectroscopy. However, this subject is beyond the scope of the present study.

Figure 21 gives plots of $\log N_l/\sigma$ vs $T - T_{NI}$ at $\dot{\gamma} = 0.1 \text{ s}^{-1}$ for eight PSHQ n moieties synthesized in this study. Earlier, it was suggested¹⁸ that at a given value of $\dot{\gamma}$, the N_l/σ ratio be used to assess elastic effects of different polymers. Interestingly enough, Figure 21 shows that (1) the N_l/σ ratio in the nematic region is very high (ca. 10) and it decreases precipitously at a temperature near T_{NI} , (2) the N_l/σ ratio in the isotropic region is negligibly small, and (3) the dependence of N_l/σ on flexible spacer length and odd-even nature of flexible spacer is hardly discernible for the PSHQ n investigated in this study.

3.4. Oscillatory Shear Flow Properties of PSHQ n . Figure 22 gives plots of $\log |\eta^*|$ vs $\log \omega$ (open symbols) for PSHQ5 at 140, 150, and 180 °C, where $|\eta^*|$ is the absolute value of complex viscosity. Also given in Figure 22 are, for comparison, plots of $\log \eta$ vs $\log \dot{\gamma}$ (filled symbols) obtained from steady-state shear flow

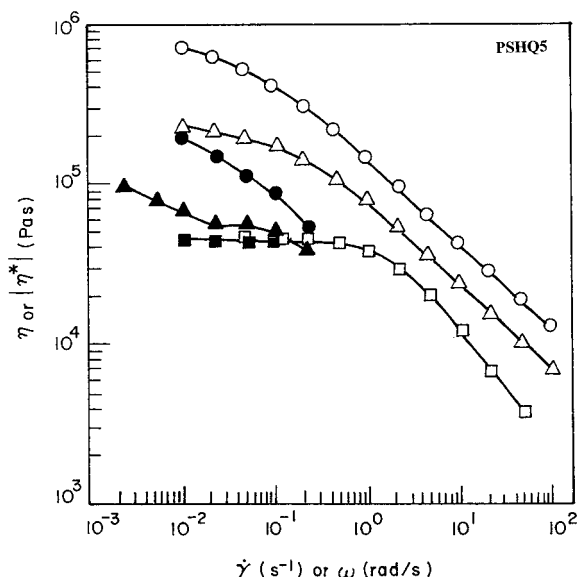


Figure 22. Plots of $\log |\eta^*|$ vs $\log \omega$ (open symbols) and $\log \eta$ vs $\log \dot{\gamma}$ (filled symbols) for PSHQ5 at various temperatures: (○, ●) 140 °C; (△, ▲) 150 °C; (□, ■) 180 °C.

experiments. The following observations are worth noting in Figure 22. (1) At 140 °C, both $\log |\eta^*|$ vs $\log \omega$ and $\log \eta$ vs $\log \dot{\gamma}$ plots show shear-thinning behavior over the entire range of ω or $\dot{\gamma}$ investigated. (2) At 150 °C, $\log |\eta^*|$ vs $\log \omega$ plots show shear-thinning behavior over the entire range of ω investigated, whereas $\log \eta$ vs $\log \dot{\gamma}$ plots show shear-thinning behavior at very low values of $\dot{\gamma}$ followed by Newtonian behavior at a narrow range of $\dot{\gamma}$, and then shear-thinning behavior again at higher $\dot{\gamma}$; i.e., a three-region viscosity curve noted first by Onogi and Asada¹⁹ is observed. (3) At 180 °C, both $\log |\eta^*|$ vs $\log \omega$ and $\log \eta$ vs $\log \dot{\gamma}$ plots show Newtonian behavior at low values of ω or $\dot{\gamma}$ and shear-thinning at higher values of ω investigated. In this study, we made observations, very similar to Figure 22, for other PSHQ n moieties synthesized.

The seemingly peculiar temperature dependence of $\log |\eta^*|$ vs $\log \omega$ and $\log \eta$ vs $\log \dot{\gamma}$ plots, given in Figure 22, can be understood by recognizing the fact that the T_{NI} of PSHQ5 is 167.7 °C (see Table 1). Namely, the viscosity curve at 180 °C is the same as that commonly observed for all homopolymers, because at 180 °C PSHQ5 is in the isotropic state. This is the reason why $\log |\eta^*|$ vs $\log \omega$ plots coincide with $\log \eta$ vs $\log \dot{\gamma}$ plots, following the Cox–Merz rule.²⁰ However, at 150 °C which is ca. 13 °C below the T_{NI} of PSHQ5, the viscosity curves no longer follow Newtonian behavior at low values of ω or $\dot{\gamma}$, because PSHQ5 is in the nematic phase, presumably containing polydomains. Notice further that at 150 °C, PSHQ5 no longer follows the Cox–Merz rule. At 140 °C which is farther away from the T_{NI} of PSHQ5, the shear-thinning behavior of viscosity persists over the entire range of ω or $\dot{\gamma}$ investigated. Similar viscosity curves were reported earlier by Kim and Han⁶ who employed PSHQ10. It is clear from Figure 22 that whether a three-region viscosity curve in a TLCP can be observed or not depends on how far away from T_{NI} its viscosities are measured.

Figure 23 gives plots of $\log G'$ vs $\log G''$ for PSHQ5 at 140, 150, and 180 °C. In the terminal region of Figure 23 we observe that (1) at 180 °C, $\log G'$ vs $\log G''$ plots have a slope of 2, which is characteristic of an isotropic (homogeneous) fluid and (2) at 140 and 150

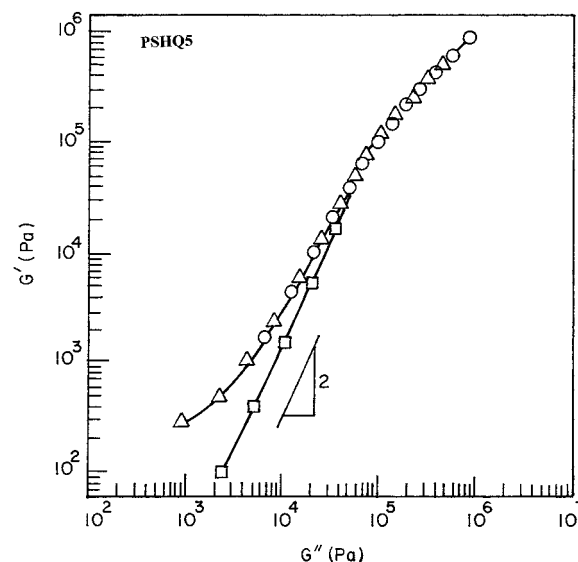


Figure 23. Plots of $\log G'$ vs $\log G''$ for PSHQ5 at various temperatures: (○) 140 °C; (△) 150 °C; (□) 180 °C.

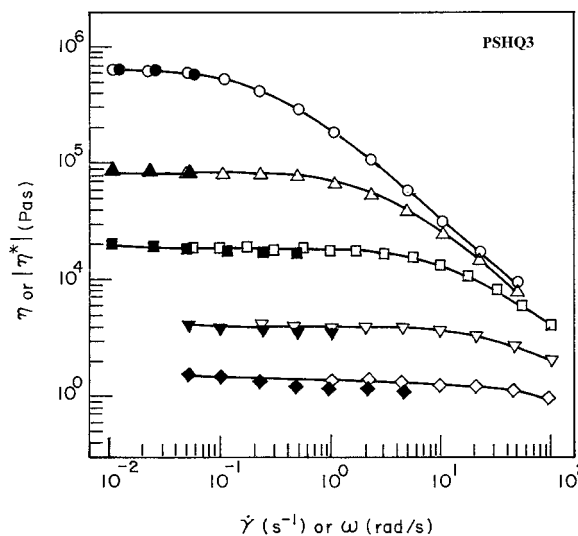


Figure 24. Plots of $\log |\eta^*|$ vs $\log \omega$ (open symbols) and $\log \eta$ vs $\log \dot{\gamma}$ (filled symbols) for PSHQ3 at various temperatures: (○, ●) 180 °C; (△, ▲) 200 °C; (□, ■) 220 °C; (▽, ▼) 240 °C; (◇, ◆) 260 °C.

°C, $\log G'$ vs $\log G''$ plots move away from that at an isotropic state. Earlier, similar observations were made by Kim and Han⁶ who employed PSHQ10. It should be mentioned that such plots were used to determine the order-disorder transition temperature of microphase-separated block copolymer.²¹ Thus we suggest that $\log G'$ vs $\log G''$ plots be used to determine the clearing temperature of TLCP. In this study, we made observations, very similar to Figure 23, for other PSHQ n moieties synthesized.

3.5. Rheological Behavior of PSHQ3. Figure 24 gives $\log |\eta^*|$ vs $\log \omega$ and $\log \eta$ vs $\log \dot{\gamma}$ plots for PSHQ3 at 180, 200, 220, 240, and 260 °C. It can be seen in Figure 24 that (i) both $\log |\eta^*|$ vs $\log \omega$ and $\log \eta$ vs $\log \dot{\gamma}$ plots exhibit Newtonian behavior at low values of $\dot{\gamma}$ or ω , (ii) the Cox–Merz rule²⁰ holds for this polymer, and (iii) the shear-thinning behavior of viscosity is observed at high values of ω . The viscosity curves of PSHQ3 at all five temperatures tested are very similar to those commonly observed in many homopolymers and, also, to the viscosity curve of PSHQ5 at 180 °C given in Figure 22. Figure 25 gives $\log G'$ vs $\log G''$

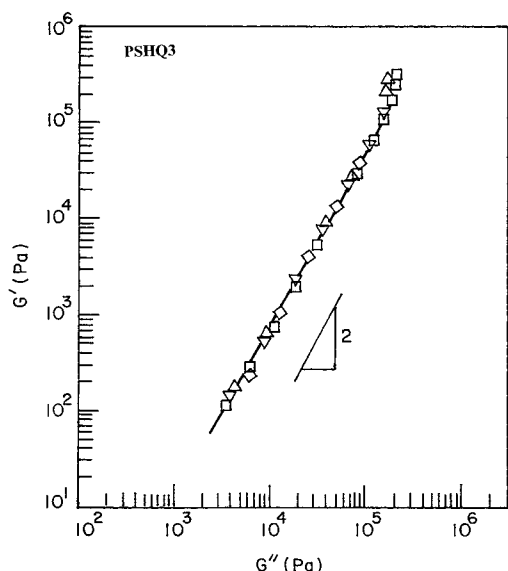


Figure 25. Plots of $\log G'$ vs $\log G''$ for PSHQ3 at various temperatures: (Δ) 200 °C; (\square) 220 °C; (∇) 240 °C; (\diamond) 260 °C.

plots for PSHQ3 at 200, 220, 240, and 260 °C, showing a single curve which is independent of temperature. Such behavior has been observed in many homopolymers^{22,23} and block copolymers in the disordered state.²¹

On the basis of the observations made above in reference to Figures 24 and 25, we conclude that PSHQ3 is indeed a non-liquid-crystalline homopolyester. This conclusion is consistent with that drawn in our previous study,⁸ which was based on DSC, polarizing optical microscopy, and wide-angle X-ray diffraction.

4. Concluding Remarks

One of the difficulties with taking rheological measurements of many TLCPs lies in that their rheological properties may keep changing during experiment. Under such circumstances, it is virtually impossible to take reproducible rheological measurements unless the initial conditions (i.e., the initial morphology) can be controlled. This is particularly a serious problem when dealing with semicrystalline TLCPs which, during rheological measurements, may form via recrystallization high-temperature melting crystals after the melting of crystals. The most effective way of circumventing such a difficulty is, as shown previously by Han and coworkers,^{1,2,6} to first heat a specimen to the isotropic region in order to erase all previous thermal histories and then to cool the specimen very slowly to a preset temperature in the nematic region before commencing rheological measurements. This approach can be realized only when a specimen has a clearing temperature much lower than its thermal degradation temperature. It turns out that, for instance, a commercial TLCP, Vectra A900, has a clearing temperature very close to or higher than its thermal degradation temperature and thus it would not be possible to give a specimen thermal treatment in the isotropic region. Under such circumstances, measurements of N_1 for TLCP are of *little* rheological significance!

As a means of controlling the initial condition for transient shear of Vectra A900, Cocchini et al.¹² suggested that a specimen be presheared, so that the zero value of N_1 can be obtained. As shown previously by Han and Kim,²⁴ preshearing has a profound influence on the morphological state of a TLCP specimen and

consequently its rheological behavior. Since the rheological behavior of a TLCP depends very much on its morphological state, one must not neglect the effect of preshearing on its rheological behavior. In this paper we have demonstrated that an attainment of zero value of N_1 is not sufficient for one to claim that the initial condition of a TLCP specimen was controlled, because different thermal histories of specimens, although they may have a zero value of N_1 before a sudden shear flow is applied, can exhibit drastically different rheological responses in transient shear flow (see Figures 11–16).

In the present study we identified the factors which might contribute to a constant change of rheological properties during experiment, by varying the thermal histories of a homologous series of thermotropic polyesters, PSHQ n . For the study, we synthesized PSHQ n moieties having odd or even numbers of methylene groups, ranging from 3 to 12, as the flexible spacers and investigated their transient, steady-state or oscillatory shear flow behavior at various temperatures in the nematic region. For the rheological investigation, each specimen was first heated to the isotropic region and then cooled slowly to a preset temperature in the nematic region before rheological measurements began. This was made possible because the clearing temperature of each PSHQ n specimen was far below its thermal degradation temperature, ca. 350 °C.

In this paper, we have shown that when taking rheological measurements of semicrystalline TLCPs in the nematic region, one must choose experimental temperatures which lie above the melting point (T_m) of high-temperature melting crystals, in order to (at least) bring the normal force of a specimen to a baseline before a sudden shear flow is applied (compare Figure 10 with Figure 11). Only *positive* values of N_1 were observed in all the PSHQ n moieties synthesized, except for PSHQ3, at all temperatures and shear rates investigated. When η was plotted against $T - T_{NI}$, we found that PSHQ n moieties having odd numbers of methylene groups have higher values of η compared to PSHQ n moieties having even numbers of methylene groups as the flexible spacer. Interestingly enough, we found that PSHQ3 exhibits Newtonian behavior, showing *no* evidence of liquid crystallinity from a rheological point of view. This observation is consistent with our earlier findings, based on differential scanning calorimetry and WAXD, that PSHQ3 is a glassy, non-liquid-crystalline homopolyester.⁸

We suggest that PSHQ n be regarded as being an excellent model compound and be used for future rheological investigation of TLCP for the following reasons: (1) PSHQ n exhibits only nematic mesophase and enables one to take rheological measurements over a very wide range of temperatures and (2) PSHQ n has excellent thermal stability in that the clearing temperature (see Table 1) is far below its thermal degradation temperature (ca. 350 °C). Such a low clearing temperature allows one to control initial conditions very effectively by heating a specimen above its clearing temperature before rheological measurement begins in the nematic region. There have been numerous TLCPs synthesized but only a few have the unique features that PSHQ n has. For instance, there are many TLCPs, having relatively low clearing temperature, synthesized which exhibit smectic mesophase(s) but, due to the two-dimensional nature, would not be ideal for rheological investigation. For this reason, very few studies have been reported on the measurements of the rheological

properties of TLCPs having smectic mesophase(s).

Before closing, we would like to mention that the rheological behavior and the morphology of TLCPs during shear flow are interrelated and therefore they are inseparable insofar as correctly interpreting rheological measurements. What is most desirable is to conduct a rheo-optical investigation of TLCP, which will enable one to make simultaneous measurements of rheological properties and morphology under shear flow. This subject will be dealt with in a future publication.

Acknowledgment. We gratefully acknowledge that this study was supported in part by the National Science Foundation under Grant CTS-9320351.

References and Notes

- (1) Kim, S. S.; Han, C. D. *J. Rheol.* **1993**, *37*, 847 and references cited therein.
- (2) Han, C. D.; Chang, S.; Kim, S. S. *Mol. Cryst. Liq. Cryst.* **1994**, *254*, 335 and references cited therein.
- (3) Ober, C. K.; Jin, J.-I.; Zhou, Q.; Lenz, R. W. *Adv Polym. Sci.* **1984**, *59*, 103 and references therein.
- (4) Sirigu, A. In *Liquid Crystallinity in Polymers*; Ciferri, A., Ed.; VCH Publishers: New York, 1991; Chapter 7 and references therein.
- (5) Furukawa, A.; Lenz, R. W. *Macromol. Chem., Macromol. Symp.* **1986**, *2*, 3.
- (6) Kim, S. S.; Han, C. D. *Polymer* **1994**, *35*, 93.
- (7) Kim, S. S.; Han, C. D. *Macromolecules* **1993**, *26*, 3176.
- (8) Chang, S.; Han, C. D. *Macromolecules* **1997**, *30*, 1670.
- (9) Lin, Y. G.; Winter, H. H. *Macromolecules* **1988**, *21*, 2439; **1991**, *41*, 2877.
- (10) Grizzuti, N.; Cavella, S.; Cicarelli, P. *J. Rheol.* **1990**, *34*, 1293.
- (11) Marrucci, G.; Maffettone, P. L. *J. Rheol.* **1991**, *34*, 1217.
- (12) Cocchini, F.; Nobile, M. R.; Acierno, D. *J. Rheol.*, **1991**, *35*, 1171; **1992**, *36*, 1307.
- (13) Baek, S. G.; Magda, J.; Larson, R. G. *J. Rheol.* **1994**, *38*, 1473.
- (14) Wunder, S. L.; Ramachandran, S.; Cochanour, C. R.; Weinberg, M. *Macromolecules* **1986**, *19*, 1696.
- (15) Gonzalez, J. M.; Munoz, M. E.; Cortazar, M.; Santamaria, A.; Pena, J. J. *J. Polym. Sci., Part B: Polym. Phys.* **1990**, *28*, 1533.
- (16) Kim, S. S.; Han, C. D. *Macromolecules* **1993**, *26*, 6633.
- (17) Abe, A. *Macromolecules* **1984**, *17*, 2280.
- (18) Han, C. D. *Rheology in Polymer Processing*; Academic Press: New York, 1976; *Multiphase Flow in Polymer Processing*, Academic Press: New York, 1981.
- (19) Onogi, S.; Asada, T. In *Rheology*; Astarita, G., Marrucci, G., Nicolais, L., Eds.; Plenum: New York, 1980; p 127.
- (20) Cox, W. P.; Merz, E. H. *J. Polym. Sci.* **1958**, *28*, 619.
- (21) (a) Han, C. D.; Kim, J. *J. Polym. Sci., Polym. Phys. Ed.* **1987**, *25*, 1741. (b) Han, C. D.; Kim, J.; Kim, J. K. *Macromolecules* **1989**, *22*, 383. (c) Han, C. D.; Baek, D. M.; Kim, J. K. *Macromolecules* **1990**, *23*, 561.
- (22) (a) Han, C. D.; Lem, K. W. *Polym. Eng. Rev.* **1983**, *2*, 135. (b) Chuang, K.; Han, C. D. *J. Appl. Polym. Sci.* **1984**, *29*, 2205.
- (23) Han, C. D.; Jhon, M. S. *J. Appl. Polym. Sci.* **1986**, *32*, 3809.
- (24) Han, C. D.; Kim, S. S. *J. Rheol.* **1994**, *38*, 13.

MA9617290